# A FULL ELECTROMAGNETIC SAR IMAGE SIMULATOR FOR URBAN STRUCTURES

*J. Dellière, A. Maruani and H. Maître*

GET Télécom Paris
LTCI UMR 5141 CNRS
46 rue Barrault, 75013 Paris

*P. Benjamin, G.-P. Piau*

EADS CCR STI
12 rue Pasteur, 92152 Suresnes Cedex

**ABSTRACT**

The purpose of this work is, starting from a close tracking of the basic electromagnetic processes, to propose a simulator enabling a better understanding of the radar images of urban areas. An improved understanding of the radar images formation processes in this case, should lead to a better knowledge of the potentialities of the SAR imagery of urban areas.

We argue that finite-difference time domain method (FDTD) is a quite new and promising approach for the propagation in urban areas. In order to numerically evaluate its electromagnetic return to an active microwave sensor, a geometric and electromagnetic model of a typical element of urban structure is presented. It consists of a rectangular parallelepiped whose vertical walls form a generic angle with respect to the sensor line of flight. This parallelepiped is placed on a either smooth or rough surface, to take into account multiple scattering between buildings and terrain.

Finally, the above model is used to analyze the field backscattered from a building, as a function of the main scene parameters. In particular, the dimensions of the building and the relationship with the look angle are analyzed.

## 1. INTRODUCTION

Although human beings are now permanently living in a "bath" of Radio Frequency radiations, the way these radiations interact to produce images as in the Synthetic Aperture Radar (SAR) imaging process is still badly controlled. A great effort has been made to evaluate the quality of propagation for applications like mobile communications. They were mostly interested in energy balances. Unfortunately the imaging process is more complex, which measures the backscattered light in any position and needs to take into account not only the interaction of light and matter at any point, but also the contributions of the interferences of the many beams, directly received, reflected or diffracted by the objects of the scene.

As long as the resolution of images was of the size order of the objects of the scene, the problem was not really addressed by the Earth Observation community which was able to efficiently treat it from a statistical point of view within the generic terms of textures and speckle. So was the problem with most of the available satellite imaging SAR systems: Radarsat, ERS, ENVISAT, etc. the resolution of which was around 10 meters.

In recent years, great efforts have been made to develop radars with very high resolutions (less than 1 meter), able to consider each element of the scene (house, street, truck, ...) as several tens of pixels. The expectation was that higher resolution would provide richer information on the scene. It has often be true and high resolution may result in images amazing with details. But it is not always true and most images obtained in many human-made landscapes are still very difficult to understand. It is the case for instance in dense urban areas, where narrow streets act as light guides and multiple reflectors (balconies, gutters, antennas) interact, or in industrial areas where regular structures may create unattended diffractions and strong scatterers are likely to overcome the other signals.

In order to help the photo interpreter, a simulation system would be welcome to simulate the propagation of a microwave in a city where all the parameters would be under control of the operator. In such a system, it would be possible to measure the effect of the geometry of the buildings, or the effect of the electromagnetic properties of the walls, the roofs, the concrete or even the pieces of furnitures inside each house. It would also be possible to evaluate the role of the radar parameters in building the image.

The puprose of the simulator here presented is to allow such experiments and to provide answers to the photo-interpreter when in front of very complex situations on the role of some elements.

In order to be able to simulate phenomena attached to the basic physical components of the scene (as for instance the roughness of the walls or the geometry of the tiles), in order to predict fine effects as may be observed in the case of interferometric imaging, we decided to choose an electromagnetic approach, issued from Maxwell equations. Such an approach is very demanding in terms of computation and memory, it is also limited in its practical ability to represent very large areas, but it is the most complete. It takes into account not only the refracted waves, but also the transmitted ones. It allows to deal with the phase of waves, and therefore elegantly solves the interferometric challenge. It may easily take into account polarization.

On the contrary, most of the methods used for applications in mobile communications make use of simplified propagation schemes, suitable for very large fields as for instance ray-tracing or geometrical approaches. Recently more complex techniques, based on the Uniform Theory of Diffraction have been proposed [1, 2], able to well treat reflected light on complex scene but ingnoring interactions between rays and internal propagations. Our work is in the line of the simulator built by V. Bouland [3], but this last simulator was only able to deal with 2D objects $z = f(x)$.

## 2. FDTD SIMULATOR

### 2.1. FDTD algorithm features

In order to use FDTD, a computational domain must be established. For our application, three different domains may be isolated. A first domain covers the free space propagation from the emitter to the city. The second is the domain of interaction between waves and matter. The third one is the free space propagation from the scene to the receiver. We will be concerned mostly by domain two which will be called ”the domain” from now on, domain two and three will be be taken into account in section 2.3. This domain is simply the physical region over which the simulation will be performed. The FDTD algorithm is based on the Yee’s scheme [4]. It discretizes with appropriate interlaced meshings, Maxwell-Faraday’s and Maxwell-Ampere’s equations, in both time and space coordinates. The vector components of the E-field and H-field are spatially staggered about cubic unit cells of the Cartesian computational domain so that each E-field vector component is located midway between a pair of H-field vector components, and conversely (Fig. 1).

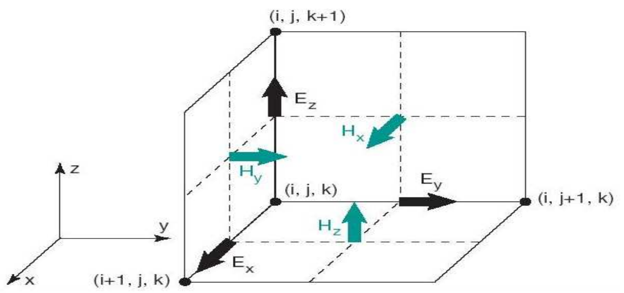


**Fig. 1**. *The standard Yee lattice used for FDTD, in which different field components use different locations in a grid.*

Contrary to other technics, such as ray-tracing method, finite element method or moment method, no approximation is necessary upstream of the spatial and temporal discretization.

Equations solver quality is guaranteed by the principles described in [5]. The FDTD discrete Maxwell’s equations solution must tend to the real solution, when spatial and temporal steps tend to zero.

Furthermore, we use a leap-frog scheme [4] for marching in time, wherein the E-field and H-field updates are staggered so that E-field updates are conducted midway during each time-step between successive H-field updates, and conversely. On the plus side, this explicit time-stepping scheme avoids the need to solve simultaneous equations. It furthermore yields dissipation-free numerical wave propagation. On the minus side, this scheme mandates an upper bound on the time-step to ensure numerical stability. The stability criterion that we use, is defined by relation 1. As a result, certain classes of simulations can require many thousands of time-steps for completion.

$$\delta_t < \frac{1}{c} \frac{1}{\sqrt{(\frac{1}{\delta_x^2} + \frac{1}{\delta_y^2} + \frac{1}{\delta_z^2})}} \tag{1}$$

The FDTD method accuracy relies on the computational domain meshing. The space should be cut into small-sized cubes relative to the wavelength in a given medium. Wave propagation modeling becomes acceptable, if the spatial step is less than one-tenth of the wavelength in the particular medium. In order to limit the computational time, we consider :

$$\delta_i = \frac{\lambda}{10} \tag{2}$$

The FDTD computing area is obviously limited in space. The waves inside this area are reflected, instead of leaving the FDTD domain. It is as if the latter is surrounded by perfect conductors. The absorbing boundary condition for truncating three-dimensional FDTD meshes is the Berengers ”perfectly matched layer” (PML) technique [6].

### 2.2. CAD and meshing

Then a modelized urban scene is created by determining its dimensions, its features and its electromagnetic parameters. Each created object is defined by its geometry (due care is given, of course to sampling theorems) and its electromagnetic parameters relative permeability $\mu_r$, relative permittivity $\varepsilon_r$ and conductivity $\sigma$. The complexity of its geometry is only limited by the number of voxels and the sampling rate. The material of each cell within the computational domain must be specified. Typically, the material is either free-space (air), metal, or dielectric. Any material can be used as long as the permeability, permittivity, and conductivity are specified.

The first step is the CAD construction and the meshing. The three-dimensional cartesian domain is described by its size ($D_i$, $i = x, y$ or $z$) and the spatial step ($\delta_i$, $i = x, y$ or $z$) along the three axis. The spatial step is depending on the emitting wavelength (or rather on the smallest wavelength within the computational domain, if the incident signal has some temporal extent) :

$$D_i = N_i \delta_i \quad \text{with} \quad \delta_i = T_i \lambda \quad (i = x,\ y\ or\ z)$$

where $N_i$ is the mesh number, according to the $i$ axis and $T_i$, the discretization rate. In essence, the tridimensional grid depends on the source and also on the medium refractive index. We only consider cubic meshes : $\delta_x = \delta_y = \delta_z = 1cm$. The dimensions of the modelized scene have to stay moderate, to ensure reasonable calculation time. They can go from around one meter to several tens of meters.

Due to the stability criterion 1, the time step $\delta_t$ is linked to the model sampling frequency $f_e$, that should verify the Shannon criterion :

$$f_e = \frac{1}{\delta_t} \geq \frac{c\sqrt{3}}{\delta_x} = \frac{c10\sqrt{3}}{\lambda} \geq 10\sqrt{3}f$$

where $f$ is the wave frequency according to the meshing step.

### 2.3. Incident field characteristics

In SAR imagery, airborne or spatial radars are used. Thus, the incident field must be initialized outside the discretization domain. This requires the description of the incident field in the FDTD domain and the computation of the backscattered field outside the area. This step is necessary for the computation of the field before the PML boundary conditions are applied. Huygens principle is the basic tool for these two operations. Although the details can be rather subtle, let us just say, that a so-called Huygens surface is delimited inside the PML to compute the near-field/far-field transformation [7].

Plane wave approximation can be used with reasonable accuracy, in some cases. This approximation is guaranteed for space radars. However, its validity for air-borne radars is restricted to only a small part of the swath, on the ground. Such is the case in our simulations.

The limited dimensions of the modelized urban structures, legitimizes the use of the plane wave approximation, in simulations.

In addition, as we can simulate a very short Gaussian electromagnetic pulse, we have no need to use a frequency ramp to improve the range resolution. But a complete Radar simulation would need both the azimuth and range compression [8].

### 2.4. Performances versus complexity

The simulator's performances consists of computer storage capacity and calculation time. The main parameters of the performances estimate, are the FDTD space dimensions, in term of mesh number ($N_x$, $N_y$ and $N_z$) and the algorithm iteration number, $N_i$.

One iteration corresponds to the electromagnetic field computation in the whole space. The total time of one simulation, is determined by the algorithm iteration number $N_i$ :

$$D = N_i \delta_t$$

The iteration number depends on the FDTD space dimensions. It must be sufficient to let the wave make a "return trip" over the scene. Thus, to get some results, $N_i$ has to be greater than the minimal quantity :

$$N_{i(min)} = 2\frac{\delta_x}{\delta_t}\frac{\sqrt{N_x^2+N_y^2+N_z^2}}{c} = 2\sqrt{3(N_x^2+N_y^2+N_z^2)} \quad (3)$$

For a scene of which dimensions are $D_x = 10$ m,$D_y = 10$ m and $D_z = 5$ m and in the case of an isotropic meshing according to a spatial step of $\delta_x = 1$ cm, the minimal iterations number is $N_{i(min)} = 5196$. This minimal iteration number has to increase, if the space is composed of dielectric objects. For example, in a medium of permittivity $\varepsilon_r = 4$, the electromagnetic wave velocity is twice as low as previously. If such a medium takes up the half-space, the new minimal value for $N_i$ is :

$$N'_{i(min)} = 2(0,5\sqrt{3(N_x^2+N_y^2+N_z^2)}+0,5*2\sqrt{3(N_x^2+N_y^2+N_z^2)}) = 1,5N_{i(min)}$$

To observe multiple reflection phenomena, $N_{i(min)}$ has to increase more : $N''_{i(min)} = 2N_{i(min)}$ to observe all double reflections and $N''_{i(min)} = 3N_{i(min)}$ for all triple reflections.

At last, for a short pulse, the calculation time is lower than for an infinite sinusoidal signal which would simulate a steady state. The electromagnetic field calculation is reduced to the duration $\tau_p$ of the incident pulse over the Huygens surface.

### 2.5. Roughness modeling

In this urban environment study, it is of significant interest to take into account radio wave scattering from rough surfaces. In particular, it is important to be able to generate speckle, and to consider realistic simulated data.

Rough surface modeling is not trivial and it is the source of many publications [9, 10, 11, 12, 13]. Several numeric methods can solve such a problem. Those methods are generally asymptotic approaches such as Khirchhoff models [9, 14] or small perturbation method [15]. The latter are limited by a certain validity domain and hardly render an account of all desired observables. In addition, these methods often need excessive computational time.

Thanks to FDTD method, we propose another option to take into account rough surface scattering. We used a quick and practical way to estimate the roughness impact on the wave propagation over urban environments, using a statistic descriptive model [9].

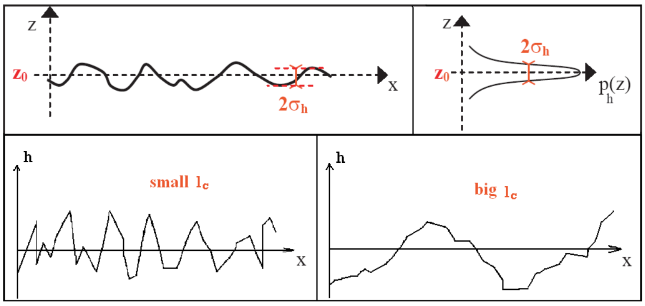


**Fig. 2**. *One rough surface example with its height density function $P_h(Z)$. For a constant $\sigma_h$, the more the correlation function grows, the more the surface behaves locally as a smooth surface.*

Height density function from one rough surface is characterized by the height mean $Z_0$, standard deviation $\sigma_h$ (that determines the height variations amplitude), the correlation width $l_c$ (that fixes the height variation regularity) and the kind of density (Gaussian, Lorentzian...).

In practice, we manually create rough surfaces with a standard CAD software. We attribute some roughness parameters to the rough surface boundary curves. The interpolation of the four boundary lines results in the rough surface. This is only an approximate approach that presents some obvious limits. It will be improved in future works.

## 3. SIMULATION GUIDANCE

The first step toward numerical electromagnetic models is to try to find sound canonical models involving simple man-made elements of urban areas. Within this framework, the radar return from a canonical structure representing a building over a rough terrain can provide useful information.

The simulator presented here is able to simulate monostatic and bistatic SAR acquisitions for a particular position of the radar. As this work set up in the SAR remote detection context, we only simulate here monostatic system specifying only one receiver placed in the same position as the source one (Fig. 3). Thus, we only consider the backscattered field towards the radar.

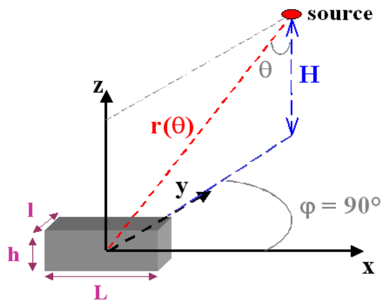


**Fig. 3**. *Spherical coordinate system used for simulations.*

The following results describe the backscattered complex signal amplitude (after quadratic demodulation and sampling as in a real SAR system [3, 13]) as a function of time. For imaging applications, and since the attenuations are not taken into account in domain one and three, the amplitude is not a relevant parameter. So amplitudes will be systematically normalized with respect to the incident field entering the domain.

## 4. RESULTS AND DISCUSSION

### 4.1. Ground modeling influence on the backscattered amplitude

In SAR imagery, the first structure to model is the ground. The ground can be considered as a horizontal plane of unlimited extent (if the image method is applied). Then the 3D grid is only constituted with studying object as a building. The ground can also be modelized by creating a finite surfacic (or volumic) plate. In this case, it must be taken into account in the computational space that makes the computation time, as long as the ground dimensions are big.

Figure 4 describes the backscattered amplitude from a finite metallic plate. Its dimensions are $5$ m $\times$ $6$ m.

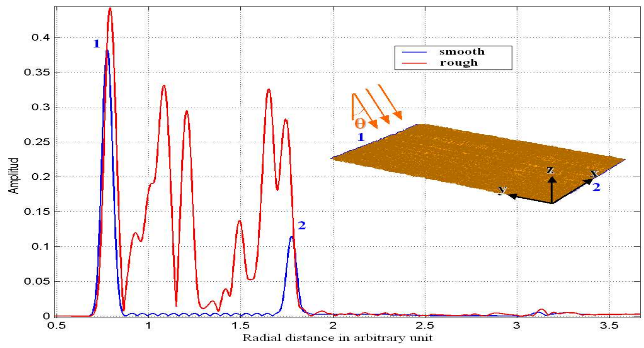


**Fig. 4**. *Backscattered amplitude from a smooth and a rough rectangular plate, in blue and red respectively. The incident direction is defined by $\theta = 40°$ and $\phi = 90°$.*

The signal backscattered by an infinite ground plane is blank, because of specular reflections whereas the one backscattered by finite metallic plate is characterized by two peaks corresponding to the ground diffracting edges. Various scenes have been modelized in order to compare backscattering from a scene composed of an infinite ground plane to scenes composed of a ground of some extent. It was shown that boundary effects can be disregarded.

Whereas the smooth ground plane only responds by two diffracting peaks, a rough ground (as proposed in section 2.5) is responding with a continuous signal with a chaotic speckle and with a greater amplitude between the two diffracting peaks.

The comparison between the two responses can be observed inside the corresponding images, with adequate quantization. Figure 5 describes a typical line of the simulated radar image. Even if the ground dimensions are not sufficient to have a good statistics, we can observe an intensity variation that appears like radar speckle.

(a) smooth (b) rough

**Fig. 5**. *Line from simulated images on smooth and rough ground, which dimensions are $5$ m $\times$ $6$ m.*

We verify the statistics of simulated data (image before azimuth compression) confirm the laws established by Goodman, in the case of a fully developed speckle. Rayleigh's law for amplitude is tendentially observed.

### 4.2. Simulations on a canonical model

Let us now focus on a canonical model. The proposed model is relevant to a building that is isolated from other man-made

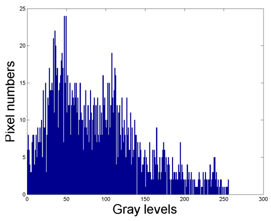


(a) Histogram

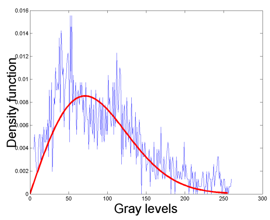


(b) Rayleigh's law

**Fig. 6**. *Histogram of the image 5 (b) and Rayleigh's law comparison.*

structures. It consists of a parallelepiped with smooth walls, surrounded by a generic ground. The scene is illuminated by a plane wave with an incident angle following the direction defined by $\theta = 40°$ and $\phi = 90°$ (see Fig. 3).

The backscattered field is interpreted as a function of the optogeometry of the scene. The backscattered field is calculated as the sum of elementary contributions from simple objects which form the whole structure. In our case, these elementary scatterers are the parallelepipeds faces and the surrounding ground.

Figure 7 shows the characteristic response of such a model. The parallelepiped dimensions are $4m \times 3m \times 1m$. It is fixed on an infinite perfect conductor smooth ground (image-method). Due to multiple reflection phenomena, the backscattered signal is characterized by high amplitude variations : it is not possible to observe simultaneously the loud and the feeble signals.

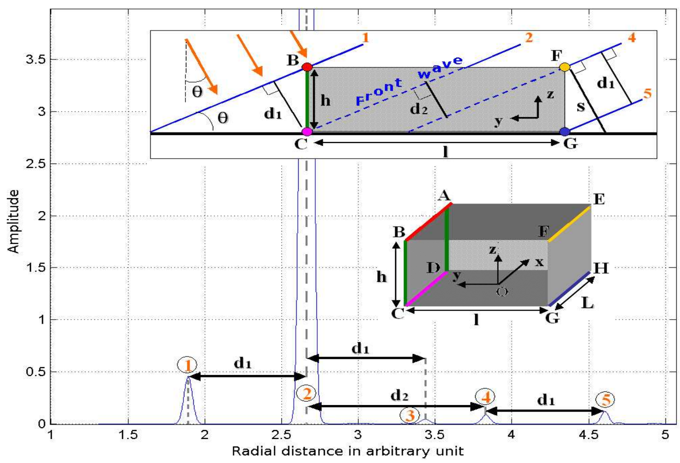


**Fig. 7**. *Backscattered signal from a parallelepiped ($4m \times 3m \times 1m$) surrounded by an infinite perfect conductor ground plane and scheme of the front wave travel inside the 3D domain. The layover dimension is $d_1 = h\cos\theta$, the shadow is characterized by $s = \frac{h}{\cos\theta}$ and $d_2 = \sin\theta(l - \frac{h}{\tan\theta})$.*

Let us focus on the main peaks of the signal. First-order contributions to the radar return are those relevant to each elementary scatterer (terrain, wall, or roof): these contributions have been widely studied in the literature and are referred to here as "single-reflection contributions" (see Fig. 8).

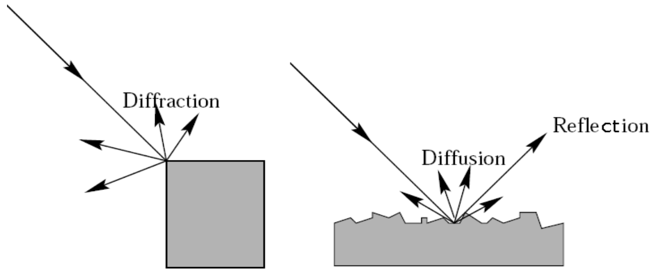


(a) First-order contributions

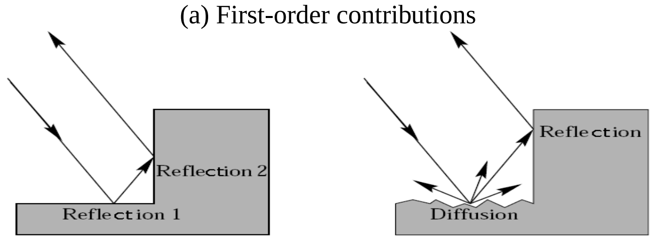


(b) Second-order contributions

**Fig. 8**. *Scheme of the first-order (a) and second-order (b) contributions.*

In the studied signal, "single-reflection contributions" appear in the first and the fourth peaks. The first one corresponds logically to the first scatterer encountered by the front wave : the diffracting edge AB, formed by the roof and the wall directly illuminated. The fourth one corresponds to the roof/wall diffracting edge EF. We can note that the amplitude of the first peak is higher than the fourth one. We made various simulations, with different configurations : whatsoever the variable parameter, we noticed that this ratio is always preserved.

We observe one second-order contribution (see Fig. 8 (b)) coming from "wall/ground reflections" and "ground/wall reflections". As expected, this peak, issued from the dihedral angle CD has a very high amplitude.

A third-order mechanism appears in the small peak 3 in the studied signal (Fig. 7). Part of the incident wave transmitted by the radar is firstly scattered by the ground towards the wall, then diffracted by the wall/roof edge AB, and finally scattered by the ground itself toward the radar (see Fig. 9).

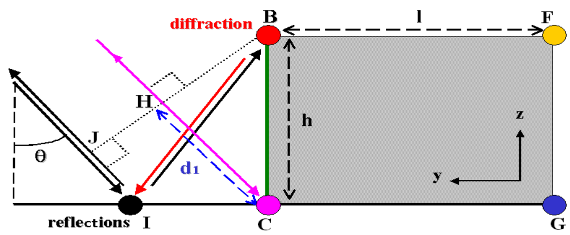


**Fig. 9**. *Representation of the third-order mechanism between the ground and the diffracting edge AB ($BI + IJ = 2HC = 2d_1$).*

Superposition of first-, second-, and third-order contributions fully represents the scattered field. Although extremly simple, this example well illustrates the complexity of radar images interpretation. We verified that the positions of the peaks in the simulation fully agree with the theory. This is still the case if the scene is more complicated. Figure 10 descibes the previous scene with a low wall in front of the parallelepiped. The backscattered signal presents quadruple reflections.

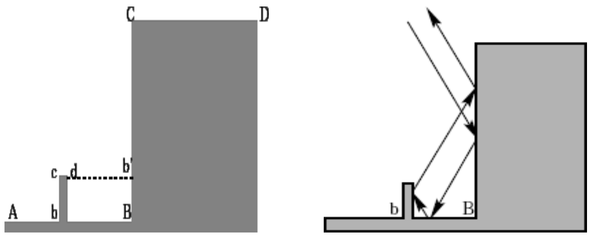


(a) scene profile (b) quadruple reflection phenomenon

**Fig. 10**. *A more complex situation with a low wall in front of a building.*

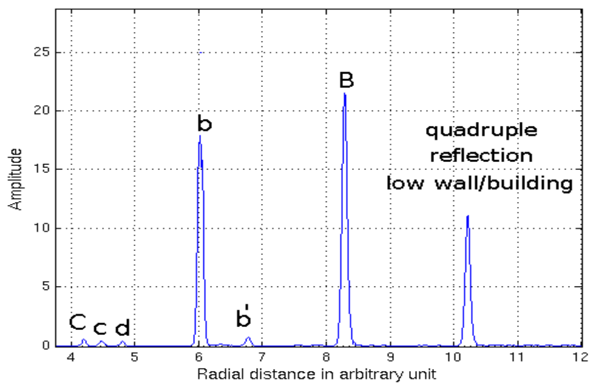


**Fig. 11**. *Backscattered signal from profile 10 (a). The signal is characterized by quadruple reflection coming after other contributions.*

## 5. CONCLUSIONS ON STRUCTURE DETECTION AND CHARACTERIZATION IN URBAN AREA

The FDTD computation provides a new approach to simulate radar wave propagation inside urban areas. It is possible to build canonical scenes, from which we can study the backscattered field as a function of the parameters of the scenes. Thanks to simulation, the role of some objects may be better understood (grids, fences, edges). The role of hidden parameters (electromagnetic characteristics of materials, internal structures of buildings,...) may be checked for. We will also soon be able to compare simulated images of real cities, digitized by conventionnal 3D cartographic means, with the obtained radar images, to extensively compare measured and expected signals.

The advantages of FDTD include : rigorous algorithm, possibility to handle dispersive materials including metals, time-domain simulation and modularity. The main disadvantage is that for many three-dimensional structures of interest to the radar community, FDTD simulation with high accuracy requires a computer memory rapidly increasing with the scene dimensions and the models meshing parameters ; the time needed to run increases consequently, in an unsustainable fahion. Todays advanced computing power enables to apply this method for SAR imagery.

## 6. ACKNOWLEDGMENTS

This study has been supported by the EADS Corporate Research Foundation.

## 7. REFERENCES

[1] G. Franceschetti, A. Iodice, D. Riccio, and G. Ruello, “SAR raw signal simulation for urban structures,” *IEEE Transactions on Geoscience and Remote Sensing*, vol. 41, no. 9, pp. 1986–1994, Sept. 2003.

[2] J. Meyer-Hilberg, “PIRDIS : A New Versatile Tool for SAR/MTI Systems Simulation,” in *EUSAR 2006*, EADS Ulm, Germany, May 2006.

[3] V. Bouland, *Caractérisation électromagnétique des milieux urbains en imagerie de télédétection par radar à synthèse d’ouverture*, Ph.D. thesis, ENST 2002E040, Oct. 2002.

[4] K.S. Yee, “Numerical solution of initial boundary value problems involving maxwell’s equations in isotropic media,” *IEEE Transactions on Antennas and Propagation*, vol. 14, no. 3, pp. 302 307, May 1966.

[5] Allen Taflove, “Review of the formulation and applications of the finite-dfference time domain method for numerical modeling of electromagnetic wave interactions with arbitrary structure,” *Wave Motion*, vol. 10, no. 6, pp. 547 582, 1988.

[6] J.P. Berenger, “A perfectly matched layer for the absorption of electromagnetics waves,” *Journal of computational physics*, vol. 114, pp. 185 200, 1994.

[7] Allen Taflove, *Advances in Computational Electrodynamics. The Finite-Difference Time-Domain Method*, Artech House, 1998.

[8] H. Maître, *Traitement des images RSO*, Hermès Science - Collection IC2, 2001, (sous la direction de).

[9] P. Beckmann and A. Spizzichino, *The scattering of electromagnetic waves from rough surfaces*, Artech House, Inc., 1963.

[10] P. Beckmann, “Scattering by non-Gaussian surfaces,” *IEEE Transactions on Antennas and Propagation*, vol. AP-21, no. 2, pp. 169–175, Mar. 1973.

[11] C. Zhiyu, Z. Dongqing, X. Minyao, and L. Zhongqian, “Separations of geometric and electromagnetic characteristics underthe kirchhoff rough surface model,” *Microwave Conference Proceedings, 1997. APMC 1997, 1997 Asia-Pacific*, vol. 3, pp. 1025–1028, Dec. 1997.

[12] G. Franceschetti, A. Iodice, and D. Riccio, “Scattering from dielectric random fractal surfaces via method of moments,” *IEEE Transactions on Geoscience and Remote Sensing*, vol. 38, no. 4, pp. 1644–1655, July 2000.

[13] C. Tison, *Interférométrie RSO à haute résolution en milieu urbain : application au calcul de MNS urbain*, Ph.D. thesis, CNES/ENST 2004E029, Nov. 2003.

[14] J. A. Ogilvy, *Theory of Wave Scattering from Random Rough Surfaces,*, Hilger, 1991.

[15] F.T. Ulaby, R. K. Moore, and A. K. Fung, *Microwave Remote Sensing : Active and Passive vol 2*, Addison-Wesley, 1982.